Journal of Technomaterial Physics
Journal homepage: https://talenta.usu.ac.id/JoTP

Reactive Diffusion Model in Determining Dissolution Rate of Edible Electronics Materials

Yuan Alfinsyah Sihombing[1]*, Asti Sawitri[2], and Marathur Rodhiyah[3]
[1)]*Department of Physics, Faculty of Mathematics and Natural Science, Universitas Sumatera Utara, Medan, 20155, Indonesia*
[2)]*Department of Physics, Universitas Halim Sanusi, Bandung, 40116, Indonesia*
[3)]*Department of Physics, Faculty of Mathematics and Natural Sciences, Universitas Sriwijaya, Sumatera Selatan, 30662, Indonesia*
*Corresponding Author: yuan@usu.ac.id

ARTICLE INFO

Article history:
Received 14 February 2026
Revised 28 February 2026
Accepted 10 March 2026
Available online 11 March 2026

E-ISSN: 2656-0755
P-ISSN: 2656-0747

How to cite:
Y. A. Sihombing, A. Sawitri, and M. Rodhiyah, "Reactive Diffusion Model in Determining Dissolution Rate of Edible Electronics Materials," Journal of Technomaterial Physics, vol. 08, no. 01, pp. 30-41, Feb. 2026, doi: 10.32734/jotp.v8i1.24766.

ABSTRACT

Edible electronic materials have emerged as an attractive research with broad potential applications. In the healthcare field, these materials can be utilized for diagnosing, monitoring, and treating organs within the gastrointestinal tract. A key characteristic of these materials is their ability to be digested and dissolved in water or bodily fluids. This study aims to theoretically investigate and predict the dissolution behavior of edible electronic materials using a one-dimensional (1D) reactive diffusion model. This model indicates that the dissolution behavior is governed by two primary parameters: the reaction rate constant (k) and the water diffusivity (D). Materials such as magnesium (Mg), zinc (Zn), and molybdenum (Mo) exhibit average dissolution rates ranging from 2.51×10^{-12} cm s^{-1} to 3.40×10^{-8} cm s^{-1} for diffusivity values between 10^{-17} and 10^{-10} cm^2 s^{-1}. In addition, the ratio of effective thickness to initial thickness (h/h_0) increases and is influenced by the molar mass of the material, following the order Mo > Zn > Mg. The dissolution rate modeling results demonstrate that the reactive diffusion model is capable of representing trends that are consistent with experimental observations.

Keywords: Diffusivity, Dissolution Rate, Edible Electronic Materials, Reactive Diffusion Model

ABSTRAK

Material elektronik yang dapat dimakan merupakan kajian yang menarik dan memiliki cakupan aplikasi yang luas. Dalam bidang kesehatan, material ini berpotensi digunakan untuk mendiagnosis, memantau, serta mengobati organ tubuh, khususnya pada saluran pencernaan. Karakteristik utama material ini adalah kemampuannya untuk dicerna serta larut dalam air atau cairan tubuh manusia. Penelitian ini bertujuan untuk menyelidiki secara teoritis dan memprediksi perilaku keterlarutan material elektronik yang dapat dimakan menggunakan model difusi reaktif satu dimensi (1D). Model ini menunjukkan bahwa laju disolusi dipengaruhi oleh dua parameter utama, yaitu konstanta laju reaksi (k) dan difusivitas air (D). Material seperti magnesium (Mg), zinc (Zn), dan molybdenum (Mo) memiliki laju disolusi rata-rata pada kisaran $2{,}51 \times 10^{-12}$ cm s^{-1} hingga $3{,}40 \times 10^{-8}$ cm s^{-1} untuk variasi difusivitas antara 10^{-17} hingga 10^{-10} cm^2 s^{-1}. Selain itu, rasio ketebalan efektif terhadap ketebalan awal (h/h_0) meningkat yang dipengaruhi oleh massa molar dari material, dengan urutan Mo > Zn > Mg. Hasil pemodelan laju disolusi ini menunjukkan bahwa model difusi reaktif mampu merepresentasikan tren yang konsisten dengan hasil eksperimen.

Kata kunci: Difusivitas, Laju Disolusi, Material Elektronik Dapat Dimakan, Model Difusi Reaktif

1. Introduction

In recent years, research in the field of electronics has advanced significantly, particularly in healthcare applications such as continuous monitoring, diagnosis, and therapeutic interventions within the human body [1], [2], [3]. Four major classes of healthcare electronics have attracted considerable attention: wearable, skin-based (epidermal), implantable, and ingestible devices [4]. In addition to functionality, electronic materials designed for biomedical applications are generally required to possess flexibility, stretchability, and transient properties to ensure safety and compatibility with biological systems [5]. Compared to implantable electronics, ingestible electronics are less invasive while offering the unique advantage of traveling through the gastrointestinal tract, enabling proximity to major organs and facilitating in situ monitoring of biomarkers as well as targeted therapeutic delivery. These characteristics make ingestible systems promising clinical tools for diagnostics and therapy [6].

Gastrointestinal disorders represent one of the most prevalent health problems worldwide. Through analysis of gastrointestinal conditions, various diseases can be diagnosed and monitored, including gastric reflux, cancer, motility disorders, varicose veins, gastritis, peptic ulcers, colorectal diseases, lactose intolerance, inflammatory bowel disease, diverticular disease, constipation, diarrhea, and irritable bowel syndrome [7], [8], [9]. The increasing prevalence of these conditions underscores the need for safe and effective ingestible electronic platforms.

Conventional ingestible electronics are typically composed of inorganic materials encapsulated within nondegradable polymeric substrates. Although functional, these systems present potential risks due to incomplete degradation or retention within the body. To minimize such risks, food-based edible electronics have emerged as a next-generation platform for diagnosis and therapy. Edible electronics are microencapsulated electronic systems composed of ingestible inorganic and organic materials that are nutritionally safe. Importantly, these devices can dissolve, degrade, and be absorbed after completing their diagnostic or therapeutic function within the gastrointestinal tract [10]. Edible electronic systems generally consist of two primary material categories: (i) materials for electronic components and (ii) materials for substrates or encapsulation layers. Electronic components can be fabricated from edible inert metals, trace elements and their oxides, edible carbon-based materials, as well as other organic food-derived materials.

The first category includes inert noble metals such as gold (Au), platinum (Pt), and silver (Ag), which exhibit excellent electrical conductivity and high biocompatibility [11], [12]. These metals are suitable for conductors, resistors, sensors, and electrodes. Due to their chemical stability, inert noble metals are minimally soluble in the gastrointestinal tract over short durations and are typically excreted from the body, with relatively low toxicity in their pure metallic form compared to their ionic salts [13].

In addition, several trace elements and their oxides possess satisfactory electrical properties, processability, acceptable solubility, and biocompatibility. Commonly studied materials include magnesium (Mg), zinc (Zn), copper (Cu), iron (Fe), silicon (Si), selenium (Se), molybdenum (Mo), silicon dioxide (SiO_2), magnesium oxide (MgO), zinc oxide (ZnO), manganese dioxide (MnO_2), and molybdenum trioxide (MoO_3) [14], [15], [16], [17]. Among these, magnesium, zinc, iron, silicon, zinc oxide, magnesium oxide, molybdenum, and silicon dioxide are frequently utilized inorganic materials in transient and edible electronic systems.

The dissolution rate of these materials can be predicted using theoretical models and validated experimentally [18]. In general, the dissolution behavior of biodegradable or transient metallic materials has been described using several theoretical approaches. Empirical kinetic models, often based on zero-order or first-order reaction rate laws, are commonly employed to estimate mass loss as a function of time under simplified assumptions of uniform surface reaction [19]. In other cases, purely diffusion-controlled models derived from Fick's laws have been applied, assuming that the rate-limiting step is the transport of water or ionic species through a boundary layer or corrosion product layer [20]. While these approaches provide useful first approximations, they typically treat interfacial reactions and mass transport separately and may not adequately capture the coupled physicochemical processes occurring simultaneously at the material–fluid interface.

Except for silicon-based materials, most inorganic components used in transient and edible electronics exhibit slightly higher dissolution rates in acidic environments than in neutral or basic conditions, a factor that is particularly relevant in the gastric environment. Although these materials can be metabolized and absorbed as essential nutrients, excessive intake resulting from uncontrolled device degradation may lead to adverse physiological effects. Therefore, understanding and controlling dissolution kinetics is crucial to ensure both safety and functional reliability.

For transient and edible electronic materials such as Mg, Zn, and Mo, dissolution is governed by coupled physicochemical processes, involving electrochemical surface reactions and inward diffusion of reactive species. This coupling makes a reaction–diffusion framework more physically representative than models that treat reaction or diffusion independently. Accordingly, a reactive diffusion model, which integrates interfacial reaction kinetics (k) with diffusion transport parameters (D), provides a more comprehensive and mechanistic description of the dissolution process.

In this study, the dissolution rate and the ratio of effective thickness to initial thickness are theoretically investigated using a one-dimensional (1D) reactive diffusion model. The edible electronic materials analyzed include magnesium (Mg), zinc (Zn), and molybdenum (Mo). This modeling approach aims to provide a predictive understanding of dissolution behavior and to evaluate its consistency with experimentally observed trends.

2. Method

One of the key properties of edible electronic materials is their dissolution behavior in solvents such as water or physiological fluids. In this study, the dissolution rate and dissolution time are determined using a reactive diffusion model. The analysis is conducted theoretically through an analytical approach to obtain a predictive description of the dissolution kinetics. The interpretation and numerical evaluation of the analytical results are subsequently performed using the Python programming language.

The dissolution process is described using a one-dimensional (1D) reactive diffusion framework. The 1D assumption is justified by considering that the lateral dimensions of the material are significantly larger than its thickness, such that mass transport and degradation predominantly occur along the thickness direction. Under this condition, spatial variations are resolved only across the thickness, enabling analytical treatment while preserving the dominant physical mechanisms governing dissolution.

Compared with surface-limited reaction models, which attribute dissolution solely to interfacial kinetics, and bulk degradation models, which assume uniform material decay without explicitly incorporating transport effects, the reactive diffusion model captures the coupled nature of the process. The theoretical foundation of this framework lies in the simultaneous coupling of water diffusion, characterized by the diffusion coefficient (D), and interfacial chemical or electrochemical reaction kinetics, described by the rate constant (k). This coupled reaction–diffusion formulation provides a mechanistic basis for the mathematical derivation presented in the following subsection.

3. Results and Discussion

3.1. Reactive Diffusion Model

The theoretical dissolution behavior of edible electronic materials can be adapted from models developed for implantable electronics. In this study, the dissolution process is described using the reactive diffusion model [21], [22], [23]. In this framework, water and hydroxide ions diffuse into the material and react simultaneously throughout the material thickness along the z-axis, as illustrated in Figure 1.

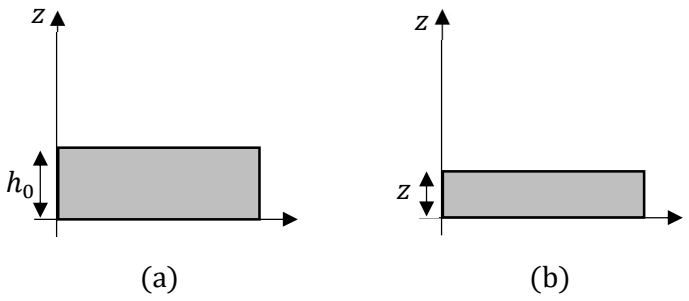

Figure 1. Material (a) before dissolution at $t = 0$ and (b) after dissolution at $t > 0$.

The diffusion equation is derived from Fick's law, which states that the mass flux of a dissolved species is proportional to the concentration gradient. It can be expressed as:

$$J = D\frac{\partial w}{\partial z} \tag{1}$$

where J is the solute flux, D is the diffusivity of the solvent (water), and w is the water concentration within the material at time t.

At time $t + \Delta t$, the rate of change of water concentration combined with the amount of water reacting with the material equals the net flux entering the system at position z. Thus,

$$\frac{\partial w}{\partial t} + kw = \frac{\partial J}{\partial z} \tag{2}$$

Substituting Eq. (1) into Eq. (2) yields:

$$\frac{\partial w}{\partial t}+kw=\frac{\partial}{\partial z}\left(D\frac{\partial w}{\partial z}\right)\rightarrow\frac{\partial w}{\partial t}+kw=D\frac{\partial^2 w}{\partial z^2} \tag{3}$$

Equation (3) represents the reactive diffusion equation, which can be written as:

$$D\frac{\partial^2 w}{\partial z^2}-kw=\frac{\partial w}{\partial t} \tag{4}$$

where k is the reaction rate constant. Assume that:

$$w=ue^{-kt} \tag{5}$$

where u is a function of position z and time t. Substituting Eq. (5) into Eq. (4) gives:

$$D\frac{\partial^2}{\partial z^2}\left[u(z,t)e^{-kt}\right]-k\left[u(z,t)e^{-kt}\right]=\frac{\partial}{\partial t}\left[u(z,t)e^{-kt}\right]$$

$$D\frac{\partial^2 u(z,t)}{\partial z^2}e^{-kt}-ku(z,t)e^{-kt}=-ku(z,t)e^{-kt}+\frac{\partial u(z,t)}{\partial t}e^{-kt}$$

$$D\frac{\partial^2 u(z,t)}{\partial z^2}=\frac{\partial u(z,t)}{\partial t} \tag{6}$$

A common method for solving Eq. (6) is to assume:

$$u=a+b \tag{7}$$

with

$$D\frac{\partial^2 a}{\partial z^2}=\frac{\partial a}{\partial t} \tag{8}$$

The boundary conditions for a are:

$$a=0, \quad \text{when } z=0 \text{ and } z=h_0$$
$$a=f(z), \quad \text{when } t=0$$

and

$$D\frac{\partial^2 b}{\partial z^2}=\frac{\partial b}{\partial t} \tag{9}$$

The boundary condition for b is:

$$b=\phi_1(t), \quad \text{when } z=0$$
$$b=\phi_2(t), \quad \text{when } z=h_0$$
$$b=0, \quad \text{when } t=0$$

Using the Laplace transform method, the solutions to Eqs. (8) and (9) are:

$$a=\frac{2}{h_0}\sum_{n=1}^{\infty}e^{-\frac{Dn^2\pi^2t}{h_0^2}}\sin\frac{n\pi z}{h_0}\int_0^{h_0}f(z')\sin\frac{n\pi z'}{h_0}dz' \tag{10}$$

$$b=\frac{2D\pi}{h_0^2}\sum_{n=1}^{\infty}ne^{-\frac{Dn^2\pi^2t}{h_0^2}}\sin\frac{n\pi z}{h_0}\int_0^{}e^{\frac{Dn^2\pi^2t}{h_0^2}}\phi_2(t)dt \tag{11}$$

Substituting Eqs. (10) and (11) into Eq. (7) yields:

$$u=\frac{2}{h_0}\sum_{n=1}^{\infty}e^{-\frac{Dn^2\pi^2t}{h_0^2}}\sin\frac{n\pi z}{h_0}\left[\int_0^{h_0}f(z')\sin\frac{n\pi z'}{h_0}dz'+\frac{nD\pi}{h_0}\int_0^{}e^{\frac{Dn^2\pi^2t}{h_0^2}}\phi_2(t)dt\right] \tag{12}$$

In the reactive diffusion model, at $t = 0$, no water has penetrated the material, such that $f(z') = 0$. This condition is referred to as zero initial water concentration. Furthermore, let $\phi_2(t) = w_0 e^{kt}$, where w_0 is the initial water concentration. Therefore, Eq. (12) becomes:

$$u = \frac{2}{h_0}\sum_{n=0}^{\infty} e^{-\frac{D(2n+1)^2\pi^2 t}{4h_0^2}} \cos\frac{(2n+1)\pi z}{2h_0}\left[\frac{(2n+1)D\pi(-1)^n}{2h_0}\int_0 e^{\frac{D(2n+1)^2\pi^2 t}{4h_0^2}} w_0 e^{kt} dt\right] \tag{13}$$

Evaluating the integral term in Eq. (13) leads to:

$$\begin{aligned}\int_0 e^{\frac{D(2n+1)^2\pi^2 t}{4h_0^2}} w_0 e^{kt} dt &= w_0 \int_0 e^{\frac{D(2n+1)^2\pi^2 t}{4h_0^2}} e^{kt} dt \\ &= w_0 \int_0 e^{\left(\frac{D(2n+1)^2\pi^2}{4h_0^2}+k\right)t} dt \\ &= w_0 \left[\frac{1}{\frac{D(2n+1)^2\pi^2}{4h_0^2}+k} e^{\left(\frac{D(2n+1)^2\pi^2 t}{4h_0^2}+k\right)t}\right]_{t=0} \\ &= -\frac{w_0}{\frac{D(2n+1)^2\pi^2}{4h_0^2}+k}\end{aligned}$$

Thus, Eq. (13) can be rewritten as:

$$u = -\frac{2}{h_0}\sum_{n=0}^{\infty} e^{-\frac{D(2n+1)^2\pi^2 t}{4h_0^2}} \cos\frac{(2n+1)\pi z}{2h_0}\left[\frac{(2n+1)D\pi(-1)^n}{2h_0}\frac{w_0}{\frac{D(2n+1)^2\pi^2}{4h_0^2}+k}\right]$$

$$= -2w_0\sum_{n=0}^{\infty} e^{-\frac{D\left(n+\frac{1}{2}\right)^2\pi^2 t}{h_0^2}} \cos\left[\left(n+\frac{1}{2}\right)\pi\frac{z}{h_0}\right]\left[\frac{\left(n+\frac{1}{2}\right)D\pi(-1)^n}{\left(n+\frac{1}{2}\right)^2\pi^2 D + kh_0^2}\right]$$

$$u = -2w_0\sum_{n=0}^{\infty}\frac{(-1)^n\left(n+\frac{1}{2}\right)\pi}{\frac{kh_0^2}{D}+\left(n+\frac{1}{2}\right)^2\pi^2} e^{-\frac{D\left(n+\frac{1}{2}\right)^2\pi^2 t}{h_0^2}} \cos\left[\left(n+\frac{1}{2}\right)\pi\frac{z}{h_0}\right] \tag{14}$$

Replacing the initial value $n = 0$ with $n = 1$ in Eq. (14) results in:

$$u = 2w_0\sum_{n=1}^{\infty}\frac{(-1)^n\left(n-\frac{1}{2}\right)\pi}{\frac{kh_0^2}{D}+\left(n-\frac{1}{2}\right)^2\pi^2} e^{-\frac{D\left(n-\frac{1}{2}\right)^2\pi^2 t}{h_0^2}} \cos\left[\left(n-\frac{1}{2}\right)\pi\frac{z}{h_0}\right] \tag{15}$$

Substituting Eq. (15) into Eq. (5) gives:

$$w = ue^{-kt}$$

$$= 2w_0 \sum_{n=1}^{\infty} \frac{(-1)^n \left(n-\frac{1}{2}\right)\pi}{\frac{kh_0^2}{D} + \left(n-\frac{1}{2}\right)^2 \pi^2} e^{-\frac{D\left(n-\frac{1}{2}\right)^2 \pi^2 t}{h_0^2}} \cos\left[\left(n-\frac{1}{2}\right)\pi \frac{z}{h_0}\right]\left(e^{-kt}\right)$$

$$= 2w_0 \sum_{n=1}^{\infty} \frac{(-1)^n \left(n-\frac{1}{2}\right)\pi}{\frac{kh_0^2}{D} + \left(n-\frac{1}{2}\right)^2 \pi^2} e^{-\left[\frac{D\left(n-\frac{1}{2}\right)^2 \pi^2}{h_0^2} + k\right] t} \cos\left[\left(n-\frac{1}{2}\right)\pi \frac{z}{h_0}\right]$$

$$w(z,t) = 2w_0 \sum_{n=1}^{\infty} \frac{(-1)^n \left(n-\frac{1}{2}\right)\pi}{\frac{kh_0^2}{D} + \left(n-\frac{1}{2}\right)^2 \pi^2} e^{-\left[\frac{kh_0^2}{D} + \left(n-\frac{1}{2}\right)^2 \pi^2\right]\frac{Dt}{h_0^2}} \cos\left[\left(n-\frac{1}{2}\right)\pi \frac{z}{h_0}\right] \tag{16}$$

When there is no water flux (zero water flux condition),

$$\left.\frac{\partial w}{\partial t}\right|_{z=0} = 0 \tag{17}$$

the reactive diffusion equation becomes:

$$D\frac{\partial^2 w}{\partial z^2} - kw = 0$$

$$\frac{\partial^2 w}{\partial z^2} - \frac{k}{D} w = 0$$

$$\frac{\partial^2 w}{\partial z^2} - \omega^2 w = 0 \tag{18}$$

where $\omega^2 = k/D$. A particular solution of Eq. (18) is:

$$w = A\cosh \omega z + B\sinh \omega z \tag{19}$$

Differentiating Eq. (19) and substituting it into Eq. (17), followed by applying the boundary condition at $z = h_0$ with $w = w_0$, yields the particular solution:

$$\frac{\partial w}{\partial t} = \omega A\sinh \omega z + \omega B\cosh \omega z$$

$$0 = \omega A\sinh \omega(0) + \omega B\cosh(0)$$

$$0 = \omega B \rightarrow B = 0$$

$$w_0 = A\cosh \omega h_0$$

$$A = \frac{w_0}{\cosh(\omega h_0)}$$

$$w = \frac{w_0}{\cosh(\omega h_0)}\cosh \omega z$$

$$w(z) = w_0 \frac{\cosh\sqrt{\frac{kz^2}{D}}}{\cosh\sqrt{\frac{kh_0^2}{D}}} \tag{20}$$

By combining Eqs. (16) and (20) as the complete solution of the reactive diffusion equation, we obtain:

$$w(z,t)=w_0\left\{\frac{\cosh\sqrt{\frac{kz^2}{D}}}{\cosh\sqrt{\frac{kh_0^2}{D}}}+2\sum_{n=1}^{\infty}\frac{(-1)^n\left(n-\frac{1}{2}\right)\pi}{\frac{kh_0^2}{D}+\left(n-\frac{1}{2}\right)^2\pi^2}e^{-\left[\frac{kh_0^2}{D}+\left(n-\frac{1}{2}\right)^2\pi^2\right]\frac{Dt}{h_0^2}}\cos\left[\left(n-\frac{1}{2}\right)\pi\frac{z}{h_0}\right]\right\} \tag{21}$$

Assuming that one mole of material reacts with q moles of water, the mass of dissolved material per unit volume along the z-axis per second is given by:

$$m'=\frac{kwM}{qM_{\text{water}}} \tag{22}$$

where m' is the mass of dissolved material in water (kg m^{-3} s^{-1}), M is the molar mass of the material (g mol^{-1}), and M_{water} is the molar mass of water (g mol^{-1}).

Substituting Eq. (21) into Eq. (22) and integrating with respect to z and t yields the dissolved material height:

$$h'=\frac{kw_0M}{q\rho M_{\text{water}}}\int_{t=0}^{t}\int_{z=0}^{h_0}\left\{\frac{\cosh\sqrt{\frac{kz^2}{D}}}{\cosh\sqrt{\frac{kh_0^2}{D}}}+2\sum_{n=1}^{\infty}\frac{(-1)^n\left(n-\frac{1}{2}\right)\pi}{\frac{kh_0^2}{D}+\left(n-\frac{1}{2}\right)^2\pi^2}e^{-\left[\frac{kh_0^2}{D}+\left(n-\frac{1}{2}\right)^2\pi^2\right]\frac{Dt}{h_0^2}}\cos\left[\left(n-\frac{1}{2}\right)\pi\frac{z}{h_0}\right]\right\}dzdt \tag{23}$$

The integral of the first term in Eq. (23) is:

$$\int_{t=0}^{t}\int_{z=0}^{h_0}\frac{\cosh\sqrt{\frac{kz^2}{D}}}{\cosh\sqrt{\frac{kh_0^2}{D}}}dzdt=\frac{\sqrt{D/kt}}{\cosh\sqrt{\frac{kh_0^2}{D}}}\sinh\sqrt{\frac{kz^2}{D}}\Bigg|_0^{h_0}=\left(\sqrt{\frac{D}{k}}t\right)\tanh\sqrt{\frac{kh_0^2}{D}} \tag{24}$$

and the integral of the second term is:

$$\int_{t=0}^{t}\int_{z=0}^{h_0}2\sum_{n=1}^{\infty}\frac{(-1)^n\left(n-\frac{1}{2}\right)\pi}{\frac{kh_0^2}{D}+\left(n-\frac{1}{2}\right)^2\pi^2}e^{-\left[\frac{kh_0^2}{D}+\left(n-\frac{1}{2}\right)^2\pi^2\right]\frac{Dt}{h_0^2}}\cos\left[\left(n-\frac{1}{2}\right)\pi\frac{z}{h_0}\right]dzdt$$

$$=2\sum_{n=1}^{\infty}\frac{(-1)^n\left(n-\frac{1}{2}\right)\pi}{\frac{kh_0^2}{D}+\left(n-\frac{1}{2}\right)^2\pi^2}\int_{t=0}^{t}\int_{z=0}^{h_0}e^{-\left[\frac{kh_0^2}{D}+\left(n-\frac{1}{2}\right)^2\pi^2\right]\frac{Dt}{h_0^2}}\cos\left[\left(n-\frac{1}{2}\right)\pi\frac{z}{h_0}\right]dzdt$$

$$=-2\sum_{n=1}^{\infty}\frac{(-1)^n h_0}{\left[\frac{kh_0^2}{D}+\left(n-\frac{1}{2}\right)^2\pi^2\right]^2}\frac{h_0^2}{D}\left[e^{-\left[\frac{kh_0^2}{D}+\left(n-\frac{1}{2}\right)^2\pi^2\right]\frac{Dt}{h_0^2}}\right]_0^t\sin\left[\left(n-\frac{1}{2}\right)\pi\frac{z}{h_0}\right]_0^{h_0}$$

$$=2\sum_{n=1}^{\infty}\frac{(-1)^n h_0}{\left[\frac{kh_0^2}{D}+\left(n-\frac{1}{2}\right)^2\pi^2\right]^2}\frac{h_0^2}{D}\left[1-e^{-\left[\frac{kh_0^2}{D}+\left(n-\frac{1}{2}\right)^2\pi^2\right]\frac{Dt}{h_0^2}}\right]\sin\left(n-\frac{1}{2}\right)\pi$$

$$=2\sum_{n=1}^{\infty}\frac{(-1)^n h_0}{\left[\frac{kh_0^2}{D}+\left(n-\frac{1}{2}\right)^2\pi^2\right]^2}\frac{h_0^2}{D}\left[1-e^{-\left[\frac{kh_0^2}{D}+\left(n-\frac{1}{2}\right)^2\pi^2\right]\frac{Dt}{h_0^2}}\right](-1)^{n+1}$$

$$= -2\sum_{n=1}^{\infty} \frac{h_0}{\left[\frac{kh_0^2}{D} + \left(n-\frac{1}{2}\right)^2 \pi^2\right]^2} \frac{h_0^2}{D} \left[1 - e^{-\left[\frac{kh_0^2}{D} + \left(n-\frac{1}{2}\right)^2 \pi^2\right]\frac{Dt}{h_0^2}}\right] \tag{25}$$

Substituting Eqs. (24) and (25) into Eq. (23) results in:

$$h' = \frac{kw_0 M}{q\rho M_{\text{water}}} \left\{ \left(\sqrt{\frac{D}{k}} t\right) \tanh\sqrt{\frac{kh_0^2}{D}} - 2\sum_{n=1}^{\infty} \frac{h_0}{\left[\frac{kh_0^2}{D} + \left(n-\frac{1}{2}\right)^2 \pi^2\right]^2} \frac{h_0^2}{D} \left[1 - e^{-\left[\frac{kh_0^2}{D} + \left(n-\frac{1}{2}\right)^2 \pi^2\right]\frac{Dt}{h_0^2}}\right] \right\}$$

$$h' = \frac{w_0 M}{q\rho M_{\text{water}}} \frac{kh_0^2}{D} \left\{ \frac{Dt}{h_0} \frac{\tanh\sqrt{\frac{kh_0^2}{D}}}{\sqrt{\frac{kh_0^2}{D}}} - 2\sum_{n=1}^{\infty} \frac{h_0 \left[1 - e^{-\left[\frac{kh_0^2}{D} + \left(n-\frac{1}{2}\right)^2 \pi^2\right]\frac{Dt}{h_0^2}}\right]}{\left[\frac{kh_0^2}{D} + \left(n-\frac{1}{2}\right)^2 \pi^2\right]^2} \right\} \tag{26}$$

where h' is the dissolved material thickness and ρ is the material density.

The remaining material thickness is then:

$$h = h_0 - h'$$

$$\frac{h}{h_0} = 1 - \frac{w_0 M}{q\rho M_{\text{water}}} \frac{kh_0^2}{D} \left\{ \frac{Dt}{h_0^2} \frac{\tanh\sqrt{\frac{kh_0^2}{D}}}{\sqrt{\frac{kh_0^2}{D}}} - 2\sum_{n=1}^{\infty} \frac{h_0 \left[1 - e^{-\left[\frac{kh_0^2}{D} + \left(n-\frac{1}{2}\right)^2 \pi^2\right]\frac{Dt}{h_0^2}}\right]}{\left[\frac{kh_0^2}{D} + \left(n-\frac{1}{2}\right)^2 \pi^2\right]^2} \right\} \tag{27}$$

To obtain the simplified expression for h/h_0, the second term in Equation (27) is neglected under the assumption that its contribution is significantly smaller than the leading term within the practical parameter regime considered in this study. Physically, this approximation corresponds to conditions in which the dissolution process is governed primarily by the dominant reaction–diffusion coupling, while higher-order correction terms introduce only minor deviations. This assumption is valid when the dimensionless parameter representing the relative strength of reaction to diffusion remains within the moderate range relevant to edible electronic materials in physiological environments. Under these conditions, the simplified form provides an accurate and analytically tractable description of thickness reduction without compromising the predictive capability of the model. So, the ratio of effective thickness to initial thickness becomes:

$$\frac{h}{h_0} \approx 1 - \frac{\sqrt{kD} w_0 M}{h_0 q\rho M_{\text{water}}} \left\{ \tanh\sqrt{\frac{kh_0^2}{D}} \right\} t$$

$$\frac{h}{h_0} \approx 1 - \frac{t}{t_c} \tag{28}$$

$$t_c = \frac{h_0 q\rho M_{\text{water}}}{\sqrt{kD} w_0 M} \tanh^{-1}\sqrt{\frac{kh_0^2}{D}} \tag{29}$$

where t_c is the critical time at which the material thickness reaches zero.

The normalized effective thickness ratio (h/h_0) provides a direct physical representation of the remaining functional material relative to its initial thickness. As dissolution progresses, the decrease in h/h_0 reflects the gradual reduction of structural and electrically active material within the device. In edible electronic systems, device performance is closely related to the integrity of conductive pathways; therefore, a critical reduction in thickness may lead to increased electrical resistance, loss of conductivity, or mechanical instability.

From a practical perspective, the temporal evolution of h/h_0 can be interpreted as an indicator of operational lifetime. When h/h_0 approaches a threshold value—below which electrical continuity or mechanical stability can no longer be maintained—the device is considered to have reached the end of its functional lifetime. Consequently, predicting h/h_0 as a function of time enables estimation of degradation duration under physiological conditions and supports rational design of edible electronic materials with controlled and programmable lifetimes.

Furthermore, the material dissolution rate can be expressed as:

$$v_{\text{dissolution}} = -\frac{dh}{dt} \approx \frac{h_0}{t_c} = \sqrt{kD}\,\frac{w_0 M}{q\rho M_{\text{water}}}\tanh\sqrt{\frac{kh_0^2}{D}} \tag{30}$$

As expressed in Eqs. (30), the dissolution rate is controlled by both transport and intrinsic material parameters, namely the diffusion coefficient (D), the interfacial reaction rate constant (k), the stoichiometric coefficient of the water–material reaction (q), the material density (ρ), the initial water concentration (w_0), the molar masses of water (M) and the material (M_{water}), and the initial thickness (h_0). The interplay among these variables defines the reaction–diffusion coupling that governs thickness reduction and material degradation over time.

3.2. Disolution Rate of Edible Electronic Materials

Inorganic materials used as components in edible electronics exhibit different dissolution rates depending on their physicochemical properties. The reactive diffusion model considers both the chemical reaction at the water/metal interface and the diffusion of water into the metal. The key parameters governing the process are the water diffusivity within the metal film (D) and the reaction rate constant (k). Since the initial thickness (h_0) is much smaller than the lateral dimensions (length and width) of the metal film, a one-dimensional (1D) model adequately captures the dissolution behavior, as discussed previously.

From Eq. (30), the two free parameters, D and k, are allowed to vary. The diffusivity D is restricted to a physically reasonable range ($\approx 10^{-17}$–10^{-10} cm^2 s^{-1}), referencing reported water diffusivity values in silica ($\approx 10^{-11}$ cm^2 s^{-1}) [24] and fused silica glass ($\approx 10^{-16}$ cm^2 s^{-1}) [25] at room temperature, since diffusivity values for water in thin metal films are generally unavailable in the literature.

The stoichiometric parameter q in Eq. (30), representing the number of moles of water reacting with one mole of material, is determined from the corresponding reaction equations:

$$\mathrm{Mg} + 2\mathrm{H_2O} \rightarrow \mathrm{Mg(OH)_2} + \mathrm{H_2} \tag{31}$$

$$\mathrm{Zn} + 2\mathrm{H_2O} \rightarrow \mathrm{Zn(OH)_2} + \mathrm{H_2} \tag{32}$$

$$2\mathrm{Mo} + 2\mathrm{H_2O} + 3\mathrm{O_2} \rightarrow 2\mathrm{H_2MoO_4} \tag{33}$$

From these reactions, the value of q is 2 for magnesium (Mg) and zinc (Zn), and 1 for molybdenum (Mo).

The relationship between diffusivity (D) and the dissolution rate of edible electronic materials (Mg, Zn, and Mo) is presented in Figure 2(a). The calculated dissolution rates range from 2.51×10^{-12} cm s^{-1} to 3.40×10^{-8} cm s^{-1} for diffusivity values between 10^{-17} and 10^{-10} cm^2 s^{-1}. Experimental studies report that magnesium forms $Mg(OH)_2$ and dissolves in deionized water at an average rate of 0.3 ± 0.1 μm h^{-1} [21], [26], while zinc forms $Zn(OH)_2$ and dissolves at 0.07 ± 0.02 μm h^{-1} under similar conditions [21], [27]. In contrast, molybdenum dissolves in water at a significantly lower rate of $(1 \pm 0.1) \times 10^{-3}$ μm h^{-1} [21], [28]. These experimental values correspond to a water diffusivity of approximately 6×10^{-12} cm^2 s^{-1} for Mg and Zn at room temperature, whereas Mo corresponds to a lower diffusivity of approximately 1×10^{-16} cm^2 s^{-1}.

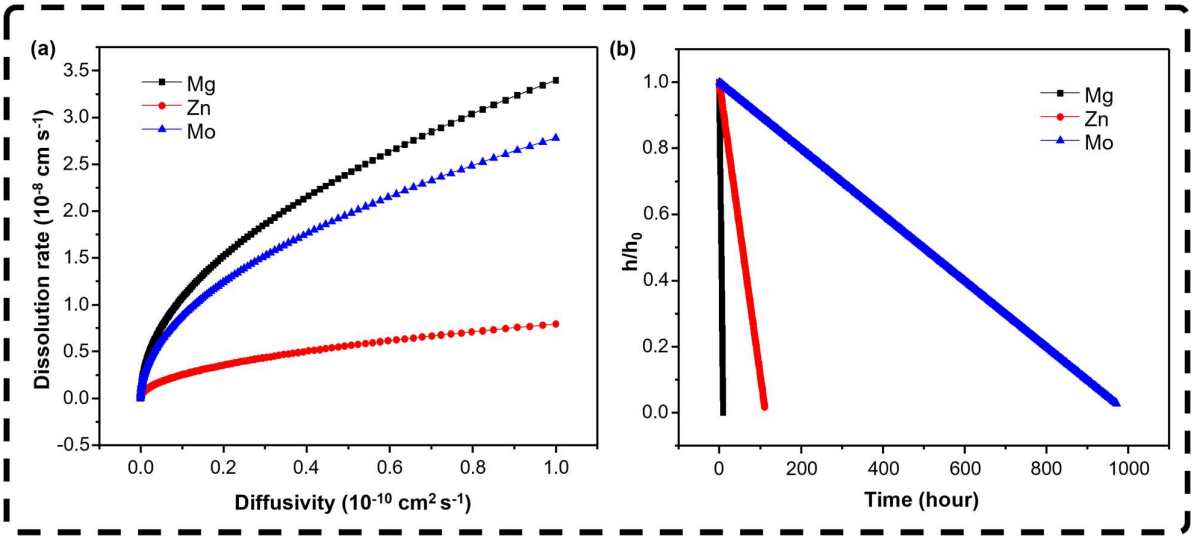

Figure 2. (a) Relationship between diffusivity and dissolution rate of edible electronic materials, and (b) ratio of effective thickness to initial thickness.

The obtained parameter values were then substituted into Eq. (28) to evaluate the ratio of effective thickness to initial thickness over time, as shown in Figure 2(b). The results indicate that Mg reacts with water and dissolves more readily than Zn and Mo. The relatively inert nature of Mo leads to a lower oxidation tendency, resulting in a significantly slower dissolution rate compared to Mg and Zn.

The dissolution behavior is governed by the coupled interaction between the diffusion coefficient (D) and the reaction rate constant (k). While D primarily controls the rate at which water penetrates into the material, k determines the intrinsic kinetics of the interfacial chemical or electrochemical reaction. The fitting results indicate that variations in D significantly influence the overall dissolution time, particularly in the diffusion-dominated regime. However, the role of k becomes increasingly important when the interfacial reaction rate approaches the same order of magnitude as the diffusion transport rate.

Physically, k reflects the material-specific reactivity in a given environment and is influenced by factors such as pH, surface condition, and electrochemical potential. For biodegradable metals such as Mg, Zn, and Mo, reported reaction rate constants in physiological environments typically fall within ranges that lead to moderate reaction–diffusion coupling, rather than purely surface-limited or purely diffusion-limited behavior. Therefore, although D is adjusted to achieve agreement with experimental dissolution trends, k remains an equally fundamental parameter that defines the intrinsic chemical responsiveness of the material.

These results confirm that the dissolution kinetics cannot be described by diffusion or reaction alone, but rather by their coupled interaction. The balance between D and k ultimately determines whether the system behaves closer to a reaction-controlled regime, a diffusion-controlled regime, or an intermediate mixed regime.

4. Conclusion

This study theoretically investigates the dissolution behavior of edible electronic materials using a one-dimensional reactive diffusion model that couples water diffusion and interfacial reaction kinetics. The analysis demonstrates that dissolution kinetics are fundamentally governed by the coupled interaction between water diffusivity (D) and the reaction rate constant (k), confirming that neither diffusion nor reaction alone can adequately describe the degradation process. The calculated dissolution rates for Mg, Zn, and Mo fall within the range of 2.51×10^{-12} to 3.40×10^{-8} cm s^{-1}, corresponding to diffusivity values between 10^{-17} and 10^{-10} cm^2 s^{-1}. Among the investigated materials, Mg shows the fastest degradation, followed by Zn and Mo, consistent with their electrochemical reactivity and oxide passivation characteristics. The evolution of the normalized effective thickness (h/h_0) further confirms this dissolution order (Mg > Zn > Mo). The reduction of h/h_0 is influenced not only by the coupled parameters D and k, but also by intrinsic material properties such as molar mass, which affect the rate of thickness loss and overall degradation dynamics. Materials with lower molar mass show more rapid thickness reduction under identical environmental conditions. Overall, the proposed reactive diffusion framework offers a predictive and mechanistic understanding of dissolution kinetics in edible electronic materials and provides a theoretical basis for designing materials with controlled degradation rates for biomedical applications.

References

[1] Y. A. Sihombing, Uperianti, D. Edikresnha, I. Anshori, D. A. Hapidin, and K. Khairurrijal, 'Screen-printed activated carbon/coconut oil/beeswax electrodes on fabrics for uric acid detection', *Mater. Chem. Phys.*, vol. 340, p. 130872, 2025, doi: 10.1016/j.matchemphys.2025.130872.

[2] A. S. Sharova, F. Melloni, G. Lanzani, C. J. Bettinger, and M. Caironi, 'Edible Electronics: The Vision and the Challenge', *Adv. Mater. Technol.*, vol. 6, no. 2, p. 2000757, 2021, doi: 10.1002/admt.202000757.

[3] Y. A. Sihombing *et al.*, 'Enhanced uric acid detection using functionalized multi-walled carbon nanotube/AgNi nanocomposites: A comparative study on screen-printed carbon electrode (SPCE) and fabric-based biosensors', *Sensors and Actuators Reports*, vol. 8, p. 100223, 2024, doi: 10.1016/j.snr.2024.100223.

[4] C. J. Bettinger, 'Materials Advances for Next-Generation Ingestible Electronic Medical Devices', *Trends Biotechnol.*, vol. 33, no. 10, pp. 575–585, 2015, doi: 10.1016/j.tibtech.2015.07.008.

[5] W. Xu *et al.*, 'Food-Based Edible and Nutritive Electronics', *Adv. Mater. Technol.*, vol. 2, no. 11, p. 1700181, 2017, doi: 10.1002/admt.201700181.

[6] C. Steiger, A. Abramson, P. Nadeau, A. P. Chandrakasan, R. Langer, and G. Traverso, 'Ingestible electronics for diagnostics and therapy', *Nat. Rev. Mater.*, vol. 4, no. 2, pp. 83–98, 2019, doi: 10.1038/s41578-018-0070-3.

[7] A. Keller, J. Pham, H. Warren, and M. In het Panhuis, 'Conducting hydrogels for edible electrodes', *J. Mater. Chem. B*, vol. 5, no. 27, pp. 5318–5328, 2017, doi: 10.1039/C7TB01247K.

[8] V. E. Balas, V. K. Solanki, and R. Kumar, *Emergence of Pharmaceutical Industry Growth with Industrial IoT Approach*. New York: Academic Press, Elsevier, 2019. doi: 10.1016/b978-0-12-819593-2.00012-1.

[9] J. Ferlay, H.-R. Shin, F. Bray, D. Forman, C. Mathers, and D. M. Parkin, 'Estimates of worldwide burden of cancer in 2008: GLOBOCAN 2008', *Int. J. Cancer*, vol. 127, no. 12, pp. 2893–2917, 2010, doi: 10.1002/ijc.25516.

[10] Y. Wu *et al.*, 'Edible and Nutritive Electronics: Materials, Fabrications, Components, and Applications', *Adv. Mater. Technol.*, vol. 5, no. 10, p. 2000100, 2020, doi: 10.1002/admt.202000100.

[11] E. Caballero-Díaz and M. V. Cases, 'Analytical methodologies for nanotoxicity assessment', *TrAC - Trends Anal. Chem.*, vol. 84, no. Part A, pp. 160–171, 2016, doi: 10.1016/j.trac.2016.03.007.

[12] Y. A. Sihombing, D. Edikresnha, I. Anshori, D. A. Hapidin, and K. Khairurrijal, 'Green-synthesized silver nanoparticles on sustainable screen-printed fabric electrode for enhanced uric acid detection', *J. Appl. Electrochem.*, vol. 56, no. 2, p. 38, 2026, doi: 10.1007/s10800-025-02385-z.

[13] B. Merchant, 'Gold, the Noble metal and the paradoxes of its toxicology', *Biologicals*, vol. 26, no. 1, pp. 49–59, 1998, doi: 10.1006/biol.1997.0123.

[14] X. Huang *et al.*, 'A Fully Biodegradable Battery for Self-Powered Transient Implants', *Small*, vol. 14, no. 28, p. 1800994, 2018, doi: 10.1002/smll.201800994.

[15] R. Mbarki, A. H. Hamzaoui, and A. Mnif, 'Dielectric properties and electrical conductivity of MgO synthesized by chemical precipitation and sol-gel method', *Eur. Phys. J. Appl. Phys.*, vol. 69, no. 1, p. 10402, 2015, doi: 10.1051/epjap/2014130287.

[16] X. Yu, W. Shou, B. K. Mahajan, X. Huang, and H. Pan, 'Materials, Processes, and Facile Manufacturing for Bioresorbable Electronics: A Review', *Adv. Mater.*, vol. 30, no. 28, p. 1707624, 2018, doi: 10.1002/adma.201707624.

[17] D. Gaspar, L. Pereira, K. Gehrke, B. Galler, E. Fortunato, and R. Martins, 'High mobility hydrogenated zinc oxide thin films', *Sol. Energy Mater. Sol. Cells*, vol. 163, pp. 255–262, 2017, doi: 10.1016/j.solmat.2017.01.030.

[18] S. W. Hwang *et al.*, 'High-performance biodegradable/transient electronics on biodegradable polymers', *Adv. Mater.*, vol. 26, no. 23, pp. 3905–3911, 2014, doi: 10.1002/adma.201306050.

[19] R. Baronas and K. Petrauskas, 'Effects of Diffusion Limitations and Partitioning on Signal Amplification and Sensitivity in Bienzyme Electrochemical Biosensors Employing Cyclic Product Conversion', *Appl. Sci.*, vol. 16, no. 3, p. 1171, 2026, doi: 10.3390/app16031171.

[20] R. Sharipov, A. Dagubayeva, G. Maldybayev, M. N. M. Ibrahim, O. Baigenzhenov, and T. Mu, 'Sustainable leaching of nickel and cobalt from asbestos waste using deep eutectic solvents: Kinetic modeling and recovery performance', *J. Hazard. Mater. Adv.*, vol. 21, p. 100948, 2026, doi: 10.1016/j.hazadv.2025.100948.

[21] L. Yin *et al.*, 'Dissolvable metals for transient electronics', *Adv. Funct. Mater.*, vol. 24, no. 5, pp. 645–658, 2014, doi: 10.1002/adfm.201301847.

[22] S. W. Hwang *et al.*, 'A physically transient form of silicon electronics', *Science (80-.).*, vol. 337, pp. 1640–1644, 2012, doi: 10.1126/science.1226325.

[23] R. Li, L. Wang, D. Kong, and L. Yin, 'Recent progress on biodegradable materials and transient electronics', *Bioact. Mater.*, vol. 3, no. 3, pp. 322–333, 2018, doi: 10.1016/j.bioactmat.2017.12.001.
[24] J. Thurn, 'Water diffusion coefficient measurements in deposited silica coatings by the substrate curvature method', *J. Non. Cryst. Solids*, vol. 354, no. 52–54, pp. 5459–5465, 2008, doi: 10.1016/j.jnoncrysol.2008.09.008.
[25] K. M. Davis and M. Tomozawa, 'Water diffusion into silica glass: Structural changes in silica glass and their effect on water solubility and diffusivity', *J. Non. Cryst. Solids*, vol. 185, no. 3, pp. 203–220, 1995, doi: 10.1016/0022-3093(95)00015-1.
[26] W. F. Ng, K. Y. Chiu, and F. T. Cheng, 'Effect of pH on the in vitro corrosion rate of magnesium degradable implant material', *Mater. Sci. Eng. C*, vol. 30, no. 6, pp. 898–903, 2010, doi: 10.1016/j.msec.2010.04.003.
[27] P. K. Bowen, J. Drelich, and J. Goldman, 'Zinc Exhibits Ideal Physiological Corrosion Behavior for Bioabsorbable Stents', *Adv. Mater.*, vol. 25, no. 18, pp. 2577–2582, 2013, doi: 10.1002/adma.201300226.
[28] W. A. Badawy and F. M. Al-Kharafi, 'Corrosion and passivation behaviors of molybdenum in aqueous solutions of different pH', *Electrochim. Acta*, vol. 44, no. 4, pp. 693–702, 1998, doi: 10.1016/S0013-4686(98)00180-7.